

# Synthesis and characterization of a clay/waterborne polyurethane nanocomposite

HSU-CHIANG KUAN, WEN-PING CHUANG, CHEN-CHI M. MA\*  
*Department of Chemical Engineering, National Tsing Hua University, HsinChu, Taiwan 300, Republic of China*  
*E-mail: ccma@che.nthu.edu.tw*

CHIN-LUNG CHIANG  
*Department of Chemical Engineering, National Tsing Hua University, HsinChu, Taiwan 300, Republic of China; Department of Industrial Safety and Health, Hung-Kuang Institute of Technology, Sha-Lu, Taiwan 433, Republic of China*

HAN-LANG WU  
*Department of Chemical Engineering, National Tsing Hua University, HsinChu, Taiwan 300, Republic of China*

A novel clay/waterborne polyurethane (WPU) nanocomposite was synthesized from polyurethane and organoclay. The clay was organically modified with a swelling agent, namely, 1,12-diaminododecane. The nanocomposite was characterized using Fourier transform infrared (FT-IR) and gel permeation chromatography (GPC). The *d*-spacing of clay was determined by X-ray diffraction (XRD) and confirmed by transmission electron microscopy (TEM). XRD and TEM analyses indicated that clay retains a layer structure in the clay/waterborne polyurethane (WPU) nanocomposite. Consequently, these materials are an intercalated nanocomposite with a *d*-spacing of around 4 to 5 nm. FT-IR revealed that adding clay does not affect the synthesis of the waterborne polyurethane. GPC results indicated that molecular weight decreased as the clay content increased. The thermal properties of the nanocomposite were examined using a thermogravimetric analyzer (TGA). Results showed that adding clay increased the temperature of thermal degradation by 15°C. © 2005 Springer Science + Business Media, Inc.

## 1. Introduction

Polymer nanocomposites containing layered structures, inorganic nanoparticles have attracted much attention for the past decade. Nanocomposites have been demonstrated with many polymers of different polarities including polyamide [1], polystyrene, polycaprolactone [2], poly (methyl methacrylate), and epoxy resin and others [1–9].

Polyurethanes are probably the most versatile class of polymers due to the great variety of raw materials that can be used in their formation. The polyurethanes are usually used as adhesives, coatings, foams, and different kinds of plastics and elastomers. Conventional polyurethane composites are usually formulated by mixing with an inorganic filler. The effect of fillers on thermal and mechanical properties of polyurethane elastomer has been studied by Salih Benli [10].

Aqueous (waterborne) polyurethanes (WPU) are high performance polymers known for their excellent properties, such as abrasion resistance, hardness, flexibility, chemical and solvent resistance, gloss, and low temperature film formation [11–17]. Water dispersions,

latexes or emulsions, of polyurethane elastomers or coatings permit the application of polyurethanes from an aqueous medium. For waterborne polyurethane systems, only water evaporates during the drying process, thus rendering these systems safe with regard to the environment. They are non-toxic, non-flammable and do not generate polluted air or waste water. The stabilization of waterborne polyurethane is achieved by the inclusion of hydrophilic centers in the polymer, such as non-ionic groups, cationic groups, and anionic groups. In this study, dimethylolpropionic acid (DMPA) units incorporated in a PU backbone were converted into effective anionic sites for water dispersion by the subsequent neutralization reaction with triethylamine (TEA).

The dispersion of clay particles in a monomer of the polymer matrix can result in the formation of three types of composite materials, namely conventional composites, intercalated nanocomposites, and exfoliated nanocomposites. Exfoliated polymer-clay nanocomposites are especially desirable for improved properties because of the homogeneous dispersion of clay and huge interfacial area between polymer and clay

\*Author to whom all correspondence should be addressed.

[18–26]. The modification of clay with swelling agents in polymer/clay nanocomposites enlarges the inter-layer spacings of the silicate sheets and modifies the hydrophilic clay to a more hydrophobic character in order to obtain better compatibility with polymers. Eventually, it can affect the properties of the final products.

This study presents the synthesis of nanocomposites from waterborne polyurethane and layered clay. Waterborne polyurethane disperses in water solution; so hydrophilic clay would be dispersed more stably in waterborne polyurethanes than in solvent-based polyurethanes. Several characterizations and property measurements of such a nanocomposite were also made in this study.

## 2. Experimental

### 2.1. Materials

Clay (Na<sup>+</sup>-Saponite) was obtained from Katamine Co., Japan. Swelling agent 1,12-diaminododecane was supplied by Tokyo Chemical Industry Co., Ltd., Tokyo, Japan. The 3-isocyanatomethyl-3,5,5-trimethylcyclohexylisocyanate (IPDI) was purchased from TCI Co., Japan. Neopentylglycol (NPG), trimethylolpropane (TMP) and dimethylol-propionic acid (DMPA) were received from the Lancaster Company, England. Polycaprolactone (PCL) with molecular weight of 1250 was obtained from Solvay Interlox Com-

pany, U.K. Triethylamine (TEA) and ethylenediamine (EDA) were supplied by the Tedia Company, USA. The structures of the reagents used are shown in the Table I.

### 2.2. Preparation of organoclay

After screening Na<sup>+</sup>-Saponite clay with a sieve of 325-mesh to remove impurities, a clay having a cationic exchange capacity of 71 meq/100 g was obtained. 12-Aminolauric acid was used as the swelling agent and the chemical structure is shown in Table I. 10 g of screened Na<sup>+</sup>-Saponite clay was gradually added to an already prepared solution of the swelling agent at 60°C and vigorously stirred for 5 h. The treated Na<sup>+</sup>-Saponite clay was washed repeatedly with de-ionized water. The filtrate was titrated with 0.1 N AgNO<sub>3</sub> until no further formation of AgCl precipitated to ensure the complete removal of chloride ions. The filter cake was then placed in a vacuum oven at 80°C for 12 h. The dried cake was ground and screened with a 325-mesh sieve to obtain the organoclay.

### 2.3. Synthesis of clay/waterborne polyurethane

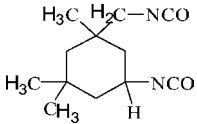
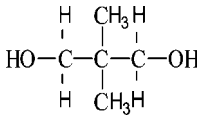
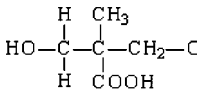
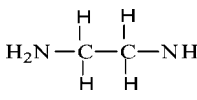
The formulation and synthesis process of the WPU is given in Fig. 1. The acetone solvent was distilled over P<sub>2</sub>O<sub>5</sub> and stored in the presence of 0.4 nm molecular sieve to keep it dry. A 500-ml round bottom, 4-necked separable glass reactor with a mechanical stirrer, thermometer, and condenser, was used in the preparation. Reaction was conducted in a N<sub>2</sub> atmosphere at constant temperature. The organoclay (0, 1, 2, 4 phr (part per hundred parts of resin)) and PCL were mixed and dried in the reactor at 120°C for 1 h. A stoichiometric mixture of IPDI, NPG, TMP, DMPA and acetone were fed into the reactor at 80°C for 6 h. The NCO-terminated prepolymer was obtained. TEA was added and stirred 30 min for neutralization. Then, the EDA/H<sub>2</sub>O solution was added and carefully controlled by a syringe pump. Small amounts of acetone (for reducing viscosity to moderate organic-water phase transfer) were removed by a rotary evaporator under reduced pressure. The nanocomposite WPU was obtained. The product was a stable PU anionomer dispersion with solids content of around 35%.

### 2.4. Characterization and property measurements

#### 2.4.1. Fourier transfer infrared spectroscopy (FT-IR)

FT-IR spectra of clay/waterborne polyurethane nanocomposite were recorded between 400–4000 cm<sup>-1</sup> with a Nicolet Avatar 320 FT-IR spectrometer, Nicolet Instrument Corporation, Madison, WI, USA. The clay/waterborne polyurethane nanocomposite sample was coated on a KBr plate. A minimum of 32 scans were averaged with a resolution of 2 cm<sup>-1</sup> within the 400–4000 cm<sup>-1</sup> range. The characteristic absorption peaks of functional group were detected and monitored during the synthesis reaction such as the N–H stretching at 3500 cm<sup>-1</sup>, O–H stretching at 3300 cm<sup>-1</sup>, NCO stretching at 2270 cm<sup>-1</sup>, C=O stretching of urethane at

TABLE I The structure of the reagents for the synthesis of the clay/waterborne polyurethane nanocomposite

Structure	Name and suppliers
$\text{H}_2\text{N}-(\text{CH}_2)_{12}-\text{NH}_2$	1,12-diaminododecane Tokyo Chemical Industry Co., Ltd., Tokyo, Japan
	Isophorone diisocyanate IPDI ( $M_w = 222.28$ ) Lancaster Company Esatgate, White Lund Morecambe, England
$\text{H}-\text{O}-(\text{CH}_2)_5-\text{C}(=\text{O})-\text{H}$	Polycaprolactone-diol ( $M_w = 1250, 1000, 830, 550$ ) PCL Aldrich Chemical Company, Milwaukee, WI, USA
	Neopentyl glycol NPG ( $M_w = 104.15$ ) Lancaster Company, Esatgate, White Lund Morecambe, England
	Dimethylol propionic acid DMPA ( $M_w = 134.13$ ) Lancaster Company Esatgate, White Lund Morecambe, England
$\text{N}(\text{C}_2\text{H}_5)_3$	Triethylene amine TEA ( $M_w = 101.19$ ) Lancaster Company Fairfield, OH (USA)
	Ethylene diamine EDA ( $M_w = 60.1$ ) Lancaster Company Fairfield, OH (USA)

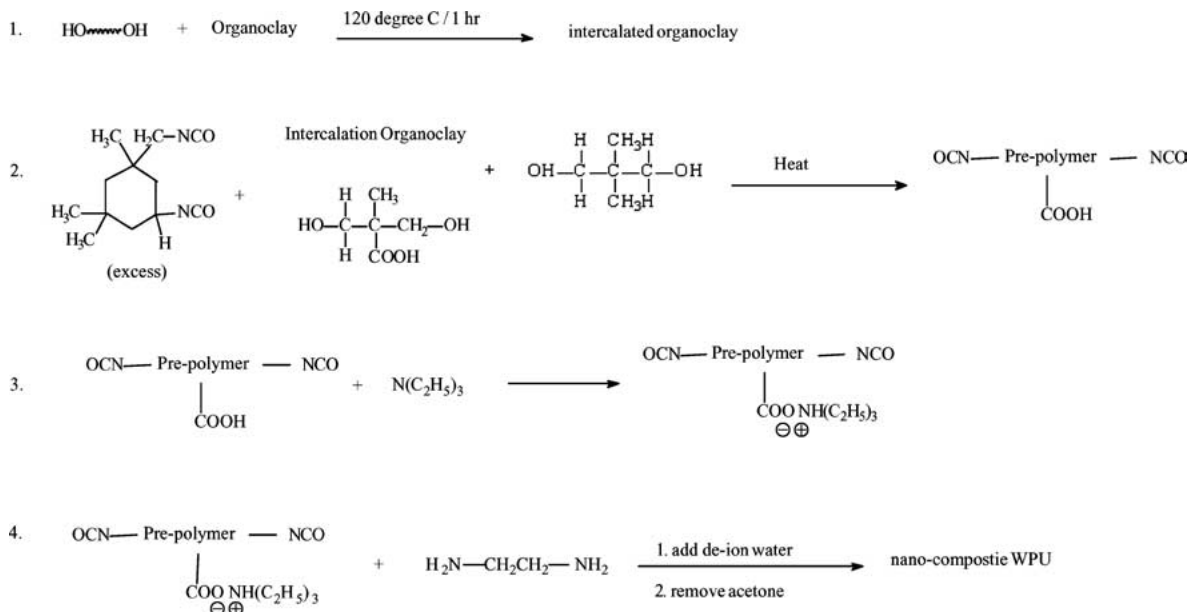


Figure 1 The synthesis process of the clay/IPDI-PCL based poly(urea-urethane)nanocomposites.

$1740 \text{ cm}^{-1}$ ,  $\text{C}=\text{O}$  stretching of urea at  $1660 \text{ cm}^{-1}$  and  $\text{Si}-\text{O}$  asymmetric stretching at  $1150 \text{ cm}^{-1}$ .

#### 2.4.2. Gel permeation chromatography (GPC)

A Waters 510 GPC (refractive index detector) with THF as the solvent was used to determine the molecular weights of the waterborne polyurethane nanocomposites (flow rate was  $10^{-6} \text{ m}^3/\text{min}$ ). The GPC calibration curves were obtained by using polystyrene standards.

#### 2.4.3. X-ray diffraction for determining the *d*-spacing of the clay

The *d*-spacing of the waterborne polyurethane nanocomposite were obtained by scanning at a rate of  $4^\circ/\text{min}$  by using a Shimadzu XD-5 X-ray diffractometer (XRD; 45 kV, 30 mA) with a copper target and scanning at a rate of  $4^\circ/\text{min}$  by using a Shimadzu XD-5 X-ray diffractometer (XRD; 45 kV, 30 mA) with a copper target and a Ni filter gives X-ray wavelength (0.1542 nm). For each interval of  $0.01^\circ$ , the diffracted X-ray intensity was recorded automatically. Samples were placed in a vacuum oven at  $40^\circ\text{C}$  for 24 h before testing. Bragg's law,  $\lambda = 2d \sin \theta$ , was used to calculate the interlayer spacing, *d*.

#### 2.4.4. Thermogravimetric analysis (TGA) analysis

Thermal degradation properties of these nanocomposites were measured by TGA (DU-Pont-951) from room temperature to  $600^\circ\text{C}$  with a heating rate of  $10^\circ\text{C}/\text{min}$  under a  $\text{N}_2$  atmosphere. The measurements were conducted using 6–10 mg samples. Weight-loss/temperature curves were recorded.

#### 2.4.5. Scanning electron microscopy (SEM) analysis

SEM analysis was performed using a JSM-5600 (Japan) model scanning electron microscope with an attached

light element detector. Electron beam energy was 15 kV. Data were collected from a scanned region of approximately  $100 \times 100$  square micrometers. The X-ray detector was operated in the thin window mode at less than 20% dead time.

#### 2.4.6. Transmission electron microscopy (TEM)

A Jeol-2000FX transmission electron microscope was utilized to investigate the morphology of nanocomposite WPU. The samples for TEM study were first prepared by placing the nanocomposite into epoxy capsules and the epoxy was cured at  $70^\circ\text{C}$  for 24 h in a vacuum oven. Then the cured epoxies containing waterborne polyurethane nanocomposite were microtomed with a Leica Ultra cut into 80–100 nm thick slices at  $-80^\circ\text{C}$ . A carbon layer 3 nm thick was deposited on these slices after mounding on 200 mesh copper grids for TEM observation.

#### 2.4.7. Atomic force microscopy (AFM)

The surface morphology of the waterborne polyurethane nanocomposites was investigated by scanning probe microscope (SPM, Digital instrument NS3a controller with D3100 stage). A fresh sample was coated on a glass substrate via spin-coating before testing. The tapping mode was used to measure the surface morphology.

### 3. Results and discussion

#### 3.1. Characterization of waterborne polyurethane

The structures of the clay/waterborne polyurethane nanocomposite coatings were analyzed by FT-IR, as shown in Fig. 2 and Table II. The characteristic peak

TABLE II The main IR absorption peaks of clay/IPDI-PCL based poly(urea-urethane) nanocomposite [27]

Functional group	Types of vibration	Wave number (cm <sup>-1</sup> )	Strength
-N=C=O	Isocyanate stretch	2275 cm <sup>-1</sup>	Broad and very strong
-C=O	Urethane stretch	1750-1700 cm <sup>-1</sup>	Very strong
-C=O	Urea stretch	1670-1640 cm <sup>-1</sup>	Very strong
-C-O	Ether stretch	1310-1000	Sharp and strong
-O-H	Alcohol stretch	3500-3200 cm <sup>-1</sup>	Very broad and very strong
-COO-H	Carboxylic acid stretch	3300-2500	Broad
-N-H	Amine stretch	1650-1500 cm <sup>-1</sup>	Sharp and strong
-C-H	Hydrocarbon stretch	3000-2800 cm <sup>-1</sup>	Sharp and medium
Si-O-Si	Asymmetric stretch	1000-1200 cm <sup>-1</sup>	Strong

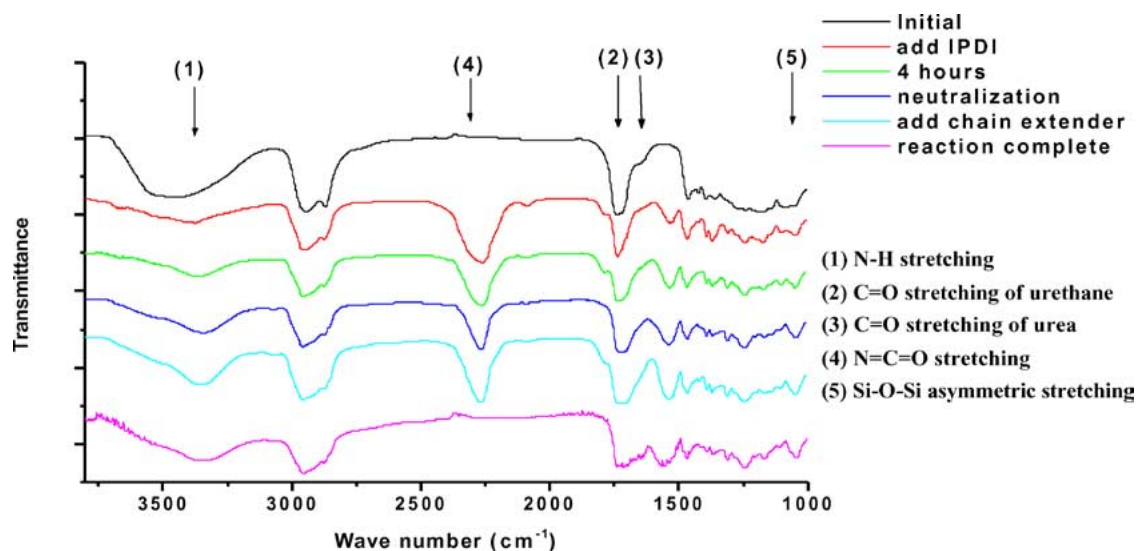


Figure 2 FT-IR spectra of the IPDI-PCL based poly(urea-urethane)/clay nanocomposite systems at various reaction steps.

of the N=C=O stretching group of IPDI at 2270 cm<sup>-1</sup> was detected during the reaction period. As the reaction proceeded, the NCO group decreased and finally disappeared completely. The C=O stretching of urea at 1640 cm<sup>-1</sup> and the C=O stretching of urethane at 1735 cm<sup>-1</sup> appeared and grew from the second step. The chain extender is DMPA. It has one equivalent -COOH group on one side, the -OH peaks become very broad (3600-2600 cm<sup>-1</sup>). In addition, the C=O stretching of -COOH group is higher than that of the C=O stretching of urethane and overlaps the C=O stretching of urethane. Therefore, the C=O stretching of urethane becomes broader and stronger.

The molecular weight of the waterborne polyurethane/clay was determined by GPC. The results in Fig. 3 indicated that the number average molecular weight ( $M_n$ ) of waterborne polyurethane synthesized herein ranged from 4000 to 12000. Fig. 3 shows that the molecular weight of the waterborne polyurethane decreased as the clay content increased. This phenomenon indicates that clay may retard the degree of polymerization of waterborne polyurethane. Clay has a layered structure, with steric hindrance and the surface hydroxy (-OH) group, it may affect the synthesis and molecular weight growth of waterborne polyurethane. Low molecular weight of waterborne polyurethane may reduce the van der Waal force between the polymer chains, reducing the mechanical properties of waterborne polyurethane.

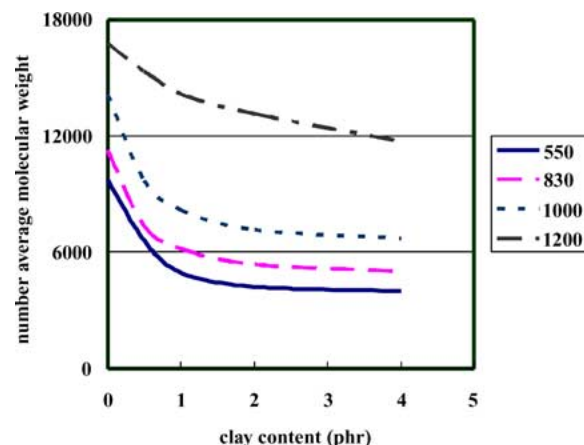


Figure 3 Number average molecular weights of clay/waterborne polyurethane nanocomposite with different soft segment molecular weights and clay contents.

### 3.2. *d*-spacing of clay/waterborne polyurethane nanocomposite

Wide Angle X-Ray Diffraction (WAXD) analysis is an effective method for examining the crystal structure of pristine clay and polymer-clay nanocomposites [1-9]. WAXD patterns show the (001) are clear diffraction peak of clay. X-ray diffraction patterns of organo-modified saponite-clay are shown in Fig. 4. According to Bragg's law,  $\lambda = 2d\sin\theta$ , the interlayer spacing (*d*-spacing) of the treated saponite-clay is 1.34 nm (that of untreated clay is 1.26 nm, as shown in Fig. 4a). Fig. 4b shows typical XRD patterns of clay/waterborne

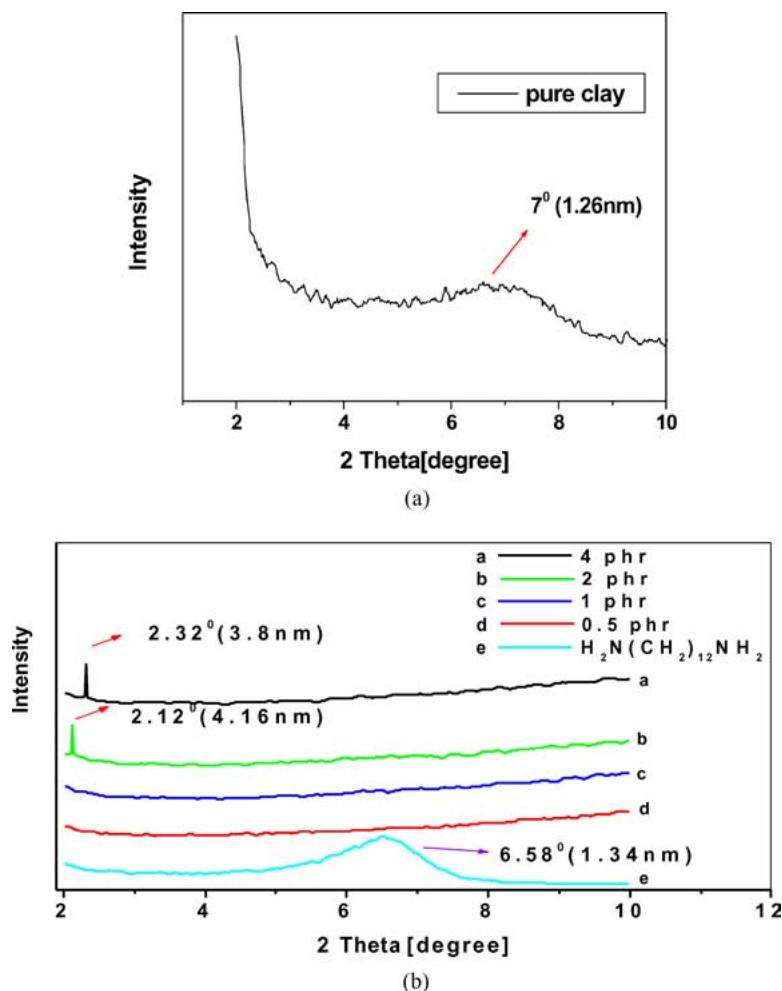


Figure 4 (a) The X-ray diffraction (XRD) pattern of pristine clay. (b) X-ray diffraction patterns of clay/waterborne polyurethane nanocomposite with different organic-saponite content from 0.5 to 4 phr.

polyurethane nano-composites, the *d*-spacing of the intercalated nanocomposite were 4.16 and 3.8 nm for clay contents 2 and 4 phr, respectively. There are no diffraction peaks in curves *c* and *d* of Fig. 4b, since the clay content is very low or these organoclays are exfoliated in waterborne polyurethane.

### 3.3. Transmission electron microscopy (TEM) micrograph of clay/waterborne polyurethane nanocomposite

TEM provided further evidence of the nano-scale dispersion of clay/waterborne polyurethane nanocomposite, as presented in Fig. 5. In the TEM cross sectional views of the 4 phr clay/WPU nanocomposite, the silicate layers were parallel to the surface of the films, and were dispersed in waterborne polyurethane. The distance between the silicate layers of organoclay in PU ranged from 4 to 10 nm, far greater than the distance between the original silicate layers of 1.5 nm.

### 3.4. Thermal properties of clay/waterborne polyurethane nanocomposite

Fig. 6 displayed the thermal decomposition behavior of pure waterborne polyurethane and clay/waterborne polyurethane nanocomposites. Results indicated that 10% weight losses of the clay/waterborne polyurethane

nanocomposite (molecular weight of soft segment was 550) with 0, 1, 2 and 4 phr clay contents were obtained at 247, 235, 245, 254 and 261°C, respectively. These results indicated that adding clay slightly increased the temperature of thermal degradation. Perhaps clay with a layered structure can retard thermal degradation. However, it may reduce the molecular weight of waterborne polyurethane. These two effects competed with each other. Consequently, the thermal degradation temperature decreased initially and then rose continuously. The thermal degradation temperature was the lowest when 0.5 phr clay was added.

### 3.5. Surface morphology of clay/waterborne polyurethane nanocomposite

Fig. 7 presents the surface topography of a clay/waterborne polyurethane nanocomposite obtained by AFM. The microphotograph showed that the mean roughness is 0.245 nm and the root mean square roughness is 0.328 nm. The surface of the clay/waterborne polyurethane nanocomposites was very smooth.

Fig. 8 shows the SEM microphotograph of clay/waterborne polyurethane nanocomposite. The length of the clay (the white region) was approximately 50–200 nm and the clay was dispersed well on the surface of the polyurethane. The microphotograph also



Figure 5 TEM microphotograph of clay/waterborne polyurethane (soft segment molecular weight 550) nanocomposite with 4 phr clay content ( $\times 100,00$ ).

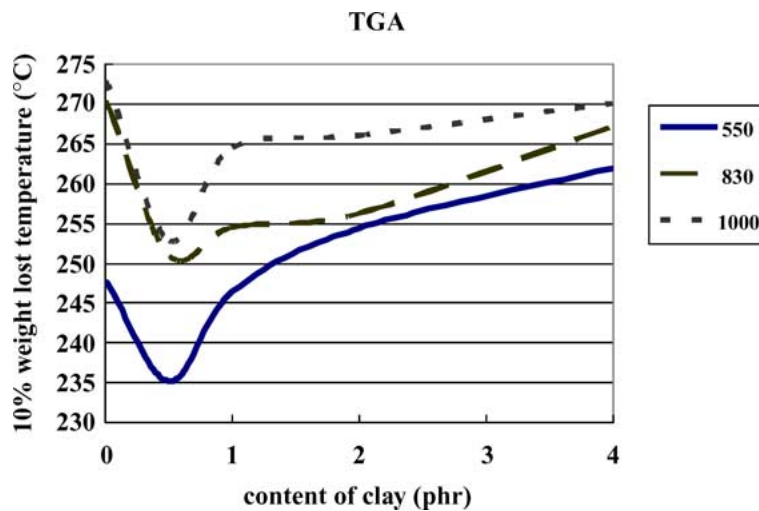


Figure 6 10% weight loss thermal degradation temperature of clay/waterborne polyurethane nanocomposite with different soft segment molecular weight and clay content.

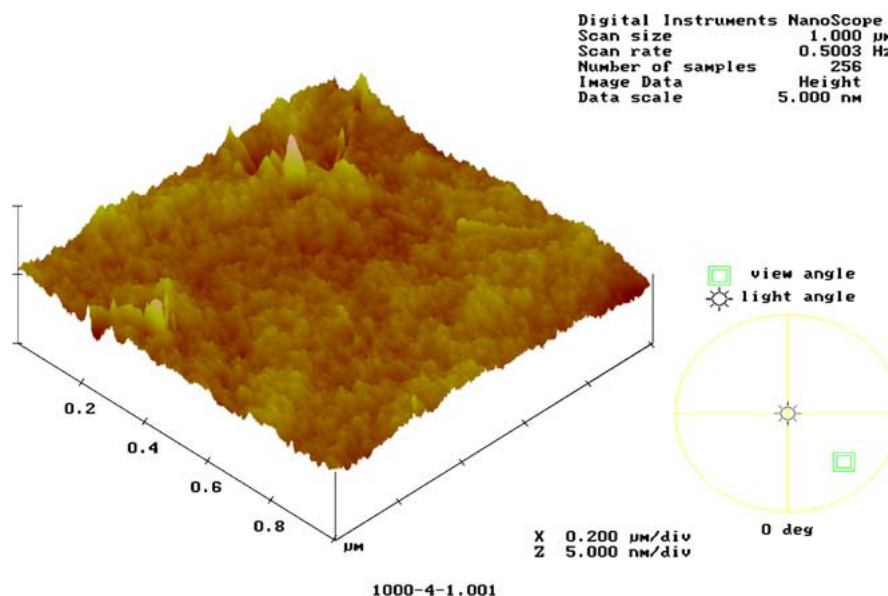


Figure 7 The AFM microphotograph of clay/waterborne polyurethane nanocomposite.

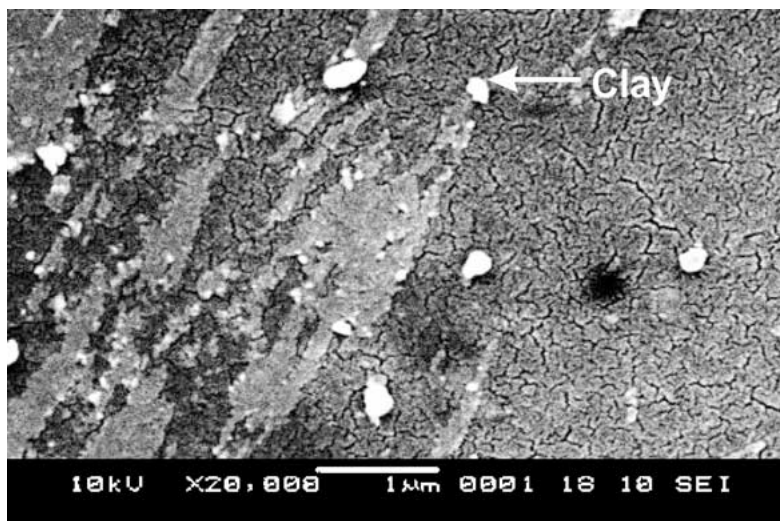


Figure 8 SEM microphotograph of the surface of waterborne polyurethane/clay nanocomposite ( $\times 20,000$ ).

indicated that clay was distributed in the deep-dark region (the region in which was located hard segment aggregation of polyurethane) mostly. A strong hydrogen bonding may exist between hard segment of waterborne polyurethane and organoclay, hence clay will distribute near the hard segment of waterborne polyurethane easier.

#### 4. Conclusions

Clay/waterborne polyurethane nanocomposites were successfully synthesized from waterborne polyurethane and organoclay. FT-IR and GPC have been used to characterize the nanocomposite. The results of molecular weight detection showed that adding clay decreased the molecular weight of waterborne polyurethane. X-ray diffraction analysis and TEM microphotography revealed that clay still retained its layered structure in the clay/waterborne polyurethane nanocomposite, that is, these materials are intercalated nanocomposites. The  $d$ -spacing of the intercalated nanocomposite is 4.16 nm. The thermal properties of the nanocomposite measured by TGA indicated that adding clay increased the temperature of thermal degradation by  $15^{\circ}\text{C}$ . AFM microphotographs showed that the surface of clay/waterborne polyurethane nanocomposites was very smooth. SEM microphotographs of clay/waterborne polyurethane nanocomposite indicated that clay was distributed in the region in which hard segment aggregation of polyurethane was located.

#### Acknowledgements

The authors would like to thank the National Science Council, Taiwan, Republic of China, for the financially supporting this research under the contract No.: NSC 91-2216-E-007-020.

#### References

1. L. P. CHENG, D. J. LIN and K. C. YANG, *J. Membrane Sci.* **172** (2000) 157.

2. G. JIMENEZ, N. OGATA, H. KAWAI and T. OGIHARA, *J. App. Polym. Sci.* **64** (1997) 2211.
3. E. P. GIANNELIS, *Adv. Mater.* **8** (1996) 29.
4. PETER C. LEBARON, ZHEN WANG and THOMAS J. PINNAVAIA, *Appl. Clay Sci.* **15** (1999) 11.
5. M. ALEXANDRE and P. DUBOIS, *Mater. Sci. Eng.* **28** (2000) 1.
6. K. J. YAO, M. SONG, D. J. HOURSTON and D. Z. LIU, *Polymer* **43** (2002) 1017.
7. T. K. CHEN, Y. I. TIEN and K. H. WEI, *J. Polym. Sci., Polym. Chem. Ed.* **37** (1999) 2225.
8. Q. WU, Z. XUE, Z. QI and F. WANG, *Polymer* **41** (2000) 2029.
9. MICHAEL J. DVORCHAK, *J. Coating Technol.* **69** (1997) 47.
10. SALIH BENLI, ULKU YILMAZER, FIKRET PEKEL and SAIM OZKAR, *J. Appl. Polym. Sci.* **68** (1998) 1057.
11. B. VOGT-BRINBRICH, *Prog. Org. Coat.* **29** (1996) 31.
12. DALE MOORE, *Adv. Mater. Proc.* **4** (1999) 31.
13. KEITH D. WEISS, *Prog. Polymer Science* **22** (1997) 203.
14. KARI-LUDWIG NOBLE, *Prog. Org. Coat.* **32** (1997) 131.
15. VOLKER DUECOFFRE, WOLFGANG DIENER, CARMEN FLOSBACH and WALTER SCHUBERT, *Prog. Org. Coat.* **34** (1998) 200.
16. CHIEN-HSIN YANG, HUEY-JIA YANG, TEN-CHIN WEN, MING-SIENG WU and JIAN-SHENG CHANG, *Polymer* **40** (1999) 871.
17. J. HUYBRECHTS, P. BRUYLANTS, A. VAES and A. DE MARRE, *Prog. Org. Coat.* **38** (2000) 67.
18. JISHENG MA, SHUFAN ZHANG and ZONGNENG QI, *J. Appl. Polym. Sci.* **82** (2001) 1444.
19. Y. HU, L. SONG, J. XU, L. YANG, Z. CHEN and W. FAN, *Colloid Polym. Sci.* **279** (2001) 819.
20. T. K. CHEN, Y. I. TIEN and K. H. WEI, *Polymer* **41** (2000) 1345.
21. ZHEN WANG and THOMAS J. PINNAVAIA, *Chem. Mater.* **10** (1998) 3769.
22. Y. HU, Z. CHEN, L. SONG, L. YANG, W. FAN and J. XU, *Colloid Polym. Sci.* **279** (2001) 819.
23. YEONG-UK AN and JIN-HAE CHANG, *IUPAC World Polym. Congr. Part (2)* (2002) 567.
24. WOO JIN CHOI and SUNG CHUL KIM, *ibid. Part (2)* (2002) 672.
25. J. W. SEO, M. S. KIM and B. K. KIM, *ibid. Part (2)* (2002) 651.
26. JIN-HAE CHANG and YEONG UK AN, *J. Polym. Sci. Polym. Phys. Ed.* **40** (2002) 670.
27. MICHAEL SZYCHER (CRC Press, New York, 1999).

Received 10 July 2003

and accepted 24 August 2004